



Cite this: *Dalton Trans.*, 2017, **46**, 7844

Stable Au^{III} complexes with four N-heterocyclic carbene groups can be prepared in high yield directly from KAuCl₄†

Ahmed H. Mageed,^{a,b} Brian W. Skelton^{a,c} and Murray V. Baker ^{*a}

Gold(III) N-heterocyclic carbene (NHC) complexes of form [Au(NHC)₄Cl₂]Cl were synthesized by reaction of KAuCl₄ with bis- and tetrakis(imidazolium) salts in the presence of a mild base. Treatment of these complexes with KPF₆ afforded four-coordinate Au^{III} complexes of form [Au(NHC)₄](PF₆)₃. X-Ray crystallography showed the [Au^{III}(NHC)₄]³⁺ cations in the hexafluorophosphate salts to have a square planar Au(NHC)₄ moiety [Au...C_{NHC} 2.024(4)–2.082(7) Å]. In the [Au^{III}(NHC)₄Cl₂]⁺ cations in the chloride salts, coordination about Au was tetragonally-distorted octahedral, the axial Au–Cl bonds being substantially longer [Au...Cl 3.148(2)–3.693(1) Å] than the equatorial Au–C_{NHC} bonds [Au...C 2.024(4)–2.082(7) Å]. NMR and conductance studies suggested that the structures of the complexes seen in the solid state persisted in DMSO solution, except in one case where a chlorido ligand dissociated from [Au^{III}(NHC)₄Cl₂]⁺ to form [Au^{III}(NHC)₄Cl]²⁺. The Au^{III}(NHC)₄ unit was surprisingly robust. An Au^{III} complex was found to undergo H/D exchange reactions in D₂O solution at 100 °C with no signs of decomposition detectable by ¹H NMR spectroscopy. ¹H NMR studies showed that various complexes containing Au^{III}(NHC)₄ moieties underwent little or no decomposition when heated at 120 °C in DMSO-d₆ for extended periods.

Received 10th April 2017,
Accepted 1st June 2017

DOI: 10.1039/c7dt01272a

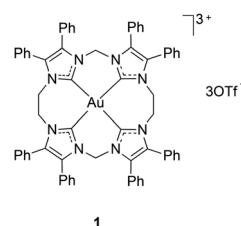
rsc.li/dalton

Introduction

Interest in gold chemistry has been growing, in part due to the promise of applications in fields of medicine, nanotechnology and catalysis.^{1–5} For example, many gold compounds have been found to inhibit cancer cell growth,^{1–3} and so gold complexes are being investigated as potential replacements for or alternatives to cisplatin in cancer chemotherapy. In this context, there has been increased research activity on the synthesis of new gold complexes involving N-heterocyclic carbene (NHC) complexes. These studies have mostly focused on mononuclear Au^I–NHC complexes, with considerably less attention being paid to Au^{III}–NHC complexes.^{6,7}

The majority of Au complexes known to date are complexes of Au^I. Synthesis of Au^{III} complexes is often problematic because of the highly oxidizing nature of Au^{III}. Attempts to synthesize Au^{III} complexes from Au^{III} salts frequently results in side-reac-

tions during which reduction of Au^{III} occurs.^{8–12} Not surprisingly, the most common synthetic pathway to Au^{III}–NHC complexes involves oxidative addition of halogens or halogen equivalents to Au^I–NHC precursor complexes.^{8,9,13–31} Other procedures, such as carbene transfer between Ag^I and Au^{III},⁸ or reaction of imidazolium ions with Au^{III} in the presence of base,^{9,10} are usually complicated by reduction of Au^{III} to Au^I. However, Lu *et al.* synthesized the Au^{III}–tetracarbene complex **1** by treatment of H[AuCl₄] with an Ag^I–NHC complex.³² Most Au^{III}–NHC complexes reported to date have square-planar Au^{III} centres with one or two NHC ligands, **1** being the only Au(NHC)₄ motif reported to date. While the Au^{III} centre in **1** is square planar, many complexes of Au^{III} with other ligands contain square pyramidal and octahedral Au centres (*e.g.* [Au(phen)(CN)₂Br] and [Au(diars)₂I₂]⁺), albeit strongly distorted, the axial metal–ligand bonds being longer than the equatorial ones.^{33,34}



^aSchool of Molecular Sciences M310, The University of Western Australia, 35 Stirling Highway, Perth, WA 6009, Australia. E-mail: murray.baker@uwa.edu.au

^bDepartment of Chemistry, Faculty of Science, The University of Kufa, P.O. Box 21, Najaf 54001, Iraq

^cCentre for Microscopy, Characterisation and Analysis M310, The University of Western Australia, Perth, WA 6009, Australia

† Electronic supplementary information (ESI) available. CCDC 1528857–1528862. For ESI and crystallographic data in CIF or other electronic format see DOI: 10.1039/c7dt01272a

In this paper, we report six new complexes containing the Au^{III}(NHC)₄ motif. The complexes were prepared simply by



treatment of KAuCl_4 with imidazolium salts in the presence of acetate. Depending on the ancillary ligands, the new complexes contain four- or six-coordinate Au^{III} centres, and all have been thoroughly characterised by NMR and X-ray studies.

Results and discussion

Synthesis of Au^{III} -NHC complexes

Au^{III} -NHC chlorido complexes $[\text{Au}(\text{L}^1)_2\text{Cl}_2]\text{Cl}$ **2**, $[\text{Au}(\text{L}^2)_2\text{Cl}_2]\text{Cl}$ **3**, and $[\text{Au}(\text{L}^3)\text{Cl}_2]\text{Cl}$ **4** (Scheme 1) were synthesized by heating KAuCl_4 with the appropriate imidazolium salt and LiOAc in DMF, following procedures we used previously to synthesize Au^{I} -NHC cyclophane complexes.¹ The complexes $[\text{Au}(\text{L}^1)_2\text{Cl}_2]\text{Cl}$ **2**, $[\text{Au}(\text{L}^2)_2\text{Cl}_2]\text{Cl}$ **3** and $[\text{Au}(\text{L}^3)\text{Cl}_2]\text{Cl}$ **4** precipitated from the mixture and were purified by recrystallisation; yields after recrystallisation were 81, 79, and 48% respectively. These yields are surprisingly high, as previous attempts to synthesize Au^{III} -NHC complexes by reaction of imidazolium salts with Au^{III} salts in the presence of base were accompanied by a substantial amount of reduction of Au^{III} to Au^{I} ,^{9,10} the problem being exacerbated by long reaction times.¹⁰ We attribute these high yields in part to remarkable stability of the Au^{III} -tetrakis(NHC) complexes (see NMR studies, below). Interestingly, the $[\text{Au}(\text{NHC})_4\text{Cl}_2]\text{Cl}$ structure seems to be the preferred product even when the stoichiometry is unfavourable—when we allowed $\text{L}^1\cdot 2\text{HCl}$ and KAuCl_4 to react in a 1 : 1 mole ratio in the presence of excess LiOAc , the only product obtained was $[\text{Au}(\text{L}^1)_2\text{Cl}_2]\text{Cl}$ **2** (86% yield based on $\text{L}^1\cdot 2\text{HCl}$). The structure of the starting imidazolium salt (*i.e.*, whether it contains a mono-, bis-, or tetrakis(imidazolium) ion) is also an important factor in determining the outcome of the reactions. The use bis- or tetrakis(imidazolium) salts as precursors makes formation of the $\text{Au}^{\text{III}}(\text{NHC})_4$ moiety kinetically favourable compared to competing processes in which $\text{Au}(\text{III})$ participates in redox reactions. When we attempted syntheses using simple monoimidazolium salts (1,3-dimethylimidazolium iodide and 1,3-diisopropylimidazolium bromide), we did not obtain any

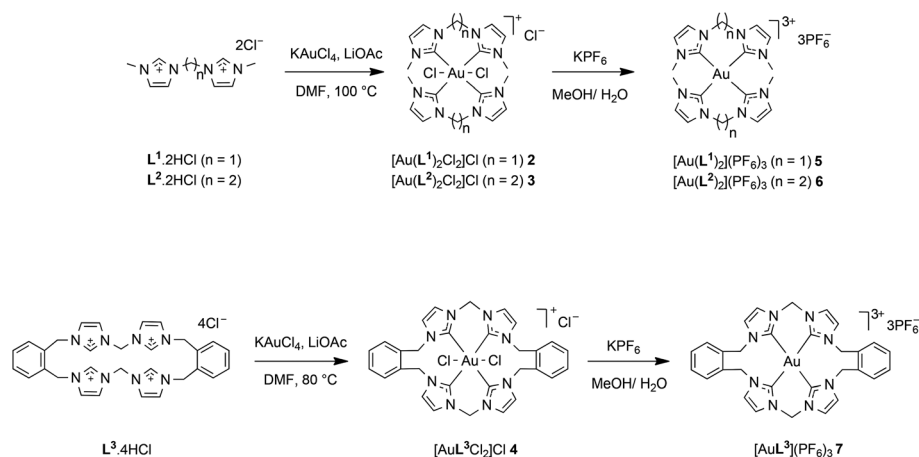
$\text{Au}^{\text{III}}(\text{NHC})_4$ -type complex, instead obtaining small amounts of $[(\text{NHC})\text{AuX}_3]$, Au^{I} -NHC complexes, and the urea-type product of oxidation of the imidazolium ion at C2. Other researchers have also reported poor results from attempts to synthesize Au^{III} complexes directly from monoimidazolium ions and Au^{III} salts in the presence of base.^{9,10}

The PF_6^- salts $[\text{Au}(\text{L}^1)_2](\text{PF}_6)_3$ **5**, $[\text{Au}(\text{L}^2)_2](\text{PF}_6)_3$ **6**, and $[\text{Au}(\text{L}^3)](\text{PF}_6)_3$ **7** were obtained from the corresponding chlorides $[\text{Au}(\text{L}^1)_2\text{Cl}_2]\text{Cl}$ **2**, $[\text{Au}(\text{L}^2)_2\text{Cl}_2]\text{Cl}$ **3**, and $[\text{Au}(\text{L}^3)\text{Cl}_2]\text{Cl}$ **4** respectively, by metathesis with KPF_6 in methanol, and were obtained as analytically-pure, white powders, in quantitative yields.

X-ray studies

Results of X-ray diffraction studies of the Au^{III} complexes are summarized in Tables 1 and 2 and Fig. 1–3. The chlorido complexes $[\text{Au}(\text{L}^1)_2\text{Cl}_2]^+$, $[\text{Au}(\text{L}^2)_2\text{Cl}_2]^+$ and $[\text{Au}(\text{L}^3)\text{Cl}_2]^+$ each contain an Au^{III} centre in a strongly distorted octahedral environment, and are examples of rarely-encountered 20-electron complexes. Removal of the chlorido ligands results in $[\text{Au}(\text{L}^1)_2]^{3+}$, $[\text{Au}(\text{L}^2)_2]^{3+}$ and $[\text{Au}(\text{L}^3)]^{3+}$, which might be thought of as structures containing commonly encountered four-coordinate Au^{III} centres (16-electron complexes), but the picture is complicated by fluorines from PF_6^- anions occupying axial coordination sites.

In each of the six complexes, the NHC units comprise an approximate square planar array around the Au^{III} centre. Au–C distances are in the range 2.024(4)–2.082(7) Å across the series of complexes, and are similar to the values seen for other complexes of form $[\text{Au}^{\text{III}}(\text{NHC})_4]^{3+}$ (**1** in Table 2),³² $[\text{Au}^{\text{III}}(\text{NHC})(\text{halide})_3]$,^{8,35} and $[\text{Au}^{\text{III}}(\text{NHC})_2(\text{halide})_2]^+$.^{8,13,35} In $[\text{Au}(\text{L}^1)_2\text{Cl}_2]\text{Cl}$ ·(MeOH)₂, $[\text{Au}(\text{L}^2)_2\text{Cl}_2]\text{Cl}$ ·(MeOH)₃, and $[\text{Au}(\text{L}^3)\text{Cl}_2]\text{Cl}$ ·(MeOH)_{3.5}, two Cl^- ligands occupy additional (axial) coordination sites, Au–Cl_{axial} being in the range 3.148(2)–3.693(1) Å, so that overall coordination geometry is distorted octahedral. These Au–Cl_{axial} bond distances are about 0.9 Å longer than Au–Cl_{equatorial} (~2.27 Å) bond lengths seen in $[\text{Au}(\text{HHCT})\text{Cl}_2]\text{AuCl}_4$ (HHCT = 1,8-bis(hydroxyethyl)-1,3,6,8,10,13-hexaazacyclotetradecane), $[\text{Au}(\text{dien})\text{Cl}_3]$ (dien = diethylenetriamine), *etc.*,^{36–38} but are much shorter



Scheme 1 Synthesis of Au^{III} -NHC complexes.



Table 1 Crystal data of new Au^{III} compounds

Complex	[AuL ¹ Cl ₂] Cl·(MeOH) ₂ 2	[AuL ² Cl ₂] Cl·(MeOH) 3	[AuL ³ Cl ₂]Cl· (MeOH) _{3.5} 4	[AuL ¹](PF ₆) ₃ · (MeCN) ₂ 5	[AuL ²](PF ₆) ₃ · (MeCN) ₂ 6	[AuL ³](PF ₆) ₃ · (MeCN) ₂ 7
Empirical formula	C ₂₀ H ₃₂ AuCl ₃ N ₈ O ₂	C ₂₁ H ₃₂ AuCl ₃ N ₈ O	C _{33.50} H ₄₂ AuCl ₃ N ₈ O _{3.50}	C ₂₂ H ₃₀ AuF ₁₈ N ₁₀ P ₃	C ₂₄ H ₃₄ AuF ₁₈ N ₁₀ P ₃	C ₃₄ H ₃₄ AuF ₁₈ N ₁₀ P ₃
Formula weight	719.85	715.86	916.07	1066.43	1094.49	1214.59
Wavelength/Å	0.71073	0.71073	1.54184	0.71073	0.71073	0.71073
Crystal system	Monoclinic	Monoclinic	Monoclinic	Monoclinic	Monoclinic	Triclinic
Space group	<i>P</i> 2 ₁ / <i>c</i>	<i>P</i> 2 ₁ / <i>c</i>	<i>I</i> 2/ <i>m</i>	<i>C</i> 2/ <i>c</i>	<i>C</i> 2/ <i>c</i>	<i>P</i> $\bar{1}$
<i>a</i> /Å	11.2465(4)	8.4520(3)	11.5286(4)	19.6697(5)	19.5075(5)	9.50080(10)
<i>b</i> /Å	12.5742(5)	21.5282(5)	18.4128(5)	11.0832(2)	11.1838(2)	15.6009(2)
<i>c</i> /Å	18.5100(7)	14.1226(4)	16.9015(6)	17.0857(6)	18.0374(4)	21.6100(3)
α /°						95.646(1)
β /°	100.893(4)	101.964(3)	98.985(3)	113.018(4)	113.442(3)	96.197(1)
γ /°						94.683(1)
<i>V</i> /Å ³	2570.44(17)	2513.88(13)	3543.7(2)	3428.18(19)	3610.39(16)	3155.08(7)
<i>Z</i>	4	4	4	4	4	3
ρ (calc)/Mg m ⁻³	1.860	1.891	1.717	2.066	2.014	1.918
μ /mm ⁻¹	6.070	6.203	10.284	4.565	4.338	3.734
Crystal size/mm ³	0.638 × 0.230 × 0.069	0.186 × 0.127 × 0.080	0.147 × 0.116 × 0.057	0.48 × 0.31 × 0.22	0.40 × 0.285 × 0.245	0.355 × 0.247 × 0.191
θ range for data collection/°	2.455 to 27.0	2.463 to 32.562	3.574 to 67.329	2.276 to 37.068	2.147 to 37.625	1.708 to 30.066
Reflections collected	24 788	31 630	17 415	31 084	43 319	71 746
Independent reflections	14 559	8553	3272	8533	9243	18 510
<i>R</i> (int)	0.1079	0.0591	0.0482	0.0436	0.0423	0.0379
Max./min. transmission	0.665 and 0.204	0.667 and 0.429	0.630 and 0.369	0.644 and 0.417	0.504 and 0.357	1.000/0.741
Restraints/parameters	0/315	0/313	166/247	0/267	12/415	0/971
Goodness-of-fit on <i>F</i> ²	1.105	1.092	1.117	1.124	1.047	1.060
<i>R</i> ₁ [<i>I</i> > 2 σ (<i>I</i>)]	0.0628	0.0460	0.0546	0.0302	0.0263	0.0252
<i>wR</i> ₂ [<i>I</i> > 2 σ (<i>I</i>)]	0.1842	0.0765	0.1430	0.0660	0.0531	0.0552
<i>R</i> ₁ (all data)	0.0712	0.0681	0.0691	0.0437	0.0475	0.0316
<i>wR</i> ₂ (all data)	0.1887	0.0819	0.1541	0.0711	0.0604	0.0576
$\Delta\rho$ (max/min)/e Å ⁻³	4.765 and -2.329	2.330 and -0.797	2.749 and -2.259	2.244 and -1.084	1.443 and -1.440	2.804 and -0.744
CCDC number	1528857	1528858	1528859	1528860	1528861	1528862

than the sum of the van der Waals radii of the atoms (~4.1 Å for Au...Cl).³⁹ This type of distorted octahedral structural motif has been reported^{34,36,38,40} in only a few cases for Au^{III} (Table S1†), and is presumably a consequence of these complexes being 20 electron complexes. For [AuL³Cl₂]Cl·(MeOH)_{3.5} 4·(MeOH)_{3.5}, the coordination of Au^{III} is broadly similar to that seen in [Au(L¹)₂Cl₂]Cl·(MeOH)₂ 2·(MeOH)₂ and [Au(L²)₂Cl₂]Cl·(MeOH) 3·(MeOH), but is complicated by the effects of solvation, the axial sites modelled as being partially occupied by chlorido ligands and solvent (methanol) molecules.

[Au(L¹)₂](PF₆)₃·(MeCN)₂ 5·(MeCN)₂ and [AuL³](PF₆)₃·(MeCN)₃ 7·(MeCN)₃ have similar coordination environments around Au to those seen in the chlorido series, but with fluorine atoms from PF₆⁻ groups occupying the axial coordination sites (Au^{III}–F 2.92(3)–3.380(2) Å). For [Au(L²)₂](PF₆)₃·(MeCN)₂ 6·(MeCN)₂, the coordination environment about Au^{III} is more strictly square planar, there being only one close contact outside the square planar array (Au^{III}–F(PF₅⁻), 3.394(2) Å), that contact not in a position that could be considered “axial”.

In the complexes containing an Au(L)₂ core (Fig. 1 and 2), the two bis(NHC) ligands (L¹ or L²) are “inverted” with respect

to each other (*i.e.*, for one ligand the methylene/ethylene linker is above the AuC₄ plane while for the other ligand the linker is below the AuC₄ plane), presumably to avoid unfavourable intramolecular interactions between the N–CH₃ groups of each ligand. A similar arrangement is seen in [AuL³]³⁺ and [AuL³Cl₂]⁺ (Fig. 3), but here the N–CH₃ groups are replaced by *o*-xylylene moieties that complete the (NHC)₄ macrocycle. Not surprisingly, the bite angle (C(11)–Au(1)–C(21)) in the complexes of L² (NHC moieties linked by CH₂CH₂) is larger than for the complexes of L¹ (NHC moieties linked by CH₂).

In each complex, the imidazolyl rings are tilted with respect to the AuC₄ coordination plane. For all complexes of L¹ and L³, in which pairs of imidazolyl units are linked by a methylene bridge, the AuC₄–imidazolyl interplanar angle is about 40°. For complexes of L², in which the imidazolyl units are linked by a longer (ethylene) bridge, the AuC₄–imidazolyl interplanar angle is higher (about 50°). This steeper inclination of the imidazolyl rings to the AuC₄ plane may be the reason why the axial Au–L bonds are longer in [Au(L²)₂Cl₂]Cl·(MeOH) 3·(MeOH) than in the other chloride salts, and absent in [Au(L²)₂](PF₆)₃·(MeCN)₂ 6·(MeCN)₂—steric hindrance from the *endo* hydrogens of the



Table 2 Selected bond lengths (Å) and angles (°) for Au^{III} cations^a

Complexes	Au–C	Au–Cl or Au–FPF ₅	C–Au–C ^b	C–Au–C ^c	Cl–Au–Cl	φ	φ'	θ	θ'
[AuL ¹ Cl ₂]Cl 2	2.040(9)	3.148(2)	85.0(4)	179.3(3)	176.78(6)	108.6(7)	—	40.6(3)	—
	2.050(9)	3.192(2)	84.5(4)	178.9(4)		109.0(7)		41.1(3)	
	2.043(9)			96.0(3)				39.8(3)	
	2.046(9)			94.5(4)				38.7(3)	
[AuL ¹]3PF ₆ 5	2.045(2)	3.380(2)	83.31(9)	180	—	108.0(2)	—	43.0(1)	—
	2.041(2)							43.7(1)	
[AuL ² Cl ₂]Cl 3	2.024(4)	3.433(1)	89.84(17)	172.65(18)	172.17(2)	—	—	54.5(2)	—
	2.054(4)	3.693(1)	91.40(18)	174.87(17)				46.7(2)	
	2.037(4)			90.52(17)				53.5(2)	
	2.061(4)			88.88(17)				46.3(2)	
[AuL ²]3PF ₆ 6	2.0402(18)	3.394(3)	88.22(8)	180	—	—	—	57.6(1)	—
	2.062(2)							48.8(1)	
[AuL ³ Cl ₂]Cl 4	2.048(8)	3.016(4)	84.5(3)	180	180	110.6(3)	109.9(7)	36.4(4)	64.3(3)
	2.082(7)			95.5(3)			109.8(7)	36.4(3)	
[AuL ³]3PF ₆ 7 (Molecule 1)	2.056(2)	3.004(5)	84.77(8)	178.57(8)	—	107.9(2)	113.0(2)	34.6(1)	74.1(1)
	2.052(2)	3.089(2)	85.63(8)	179.75(8)		107.6(2)	112.1(2)	39.4(1)	63.4(1)
	2.051(2)			94.52(8)		109.3(2)		36.8(1)	
	2.056(2)			95.08(8)		107.8(2)		35.7(1)	
(Molecule 2)	2.050(2)	2.903(4)	86.06(8)	180	—	108.1(2)	111.2(2)	36.7(1)	63.6(1)
	2.055(2)			93.94(8)		109.92(2)		36.4(1)	
1 ³²	2.017(9)	—	86.0(4)	174.5(4)	—	109.6(7)	—	29.8(3)	—
	2.042(10)		86.0(4)	174.5(4)		111.4(8)		45.3(3)	
	2.052(9)		94.4(3)					42.7(3)	
	2.030(11)		94.3(3)					33.7(4)	

^a φ = N_{NHC}–C–N_{NHC}; φ' = N_{NHC}–C–C_{arene}; θ = AuC₄/NHC inter-planar angle; θ' = AuC₄-arene inter-planar angle. ^b Angle between NHCs directly linked by CH₂ or (CH₂)₂ group. ^c Angle between NHCs not directly linked by CH₂ or (CH₂)₂ group.

ethylene bridge may inhibit approach of axial ligands to the Au centre.

UV-vis electronic absorption spectroscopy and conductance measurements

The UV-vis absorption spectra of all the Au^{III}–NHC complexes displayed intense absorption in the region λ = 230–290 nm (Fig. 4 and Table 3). We attribute these high energy absorption bands to π – π^* intraligand transitions involving the NHC ligands.³⁵ In the spectra of [Au(L¹)₂Cl₂]Cl **2** and [Au(L²)₂Cl₂]Cl **3** (but not for [AuL³Cl₂]Cl **4**) a weaker absorbance is observed in the region 300–350 nm. These weaker absorption bands have energies and molar extinction coefficients (ϵ on the order of 10^3 – 10^4 M^{–1} cm^{–1}) similar to those of ligand-to-metal-charge-transfer (LMCT) bands of the [AuCl₄][–] ion, which has been studied in detail by Mason *et al.*⁴¹ Similar absorptions were also displayed by other NHC adducts of Au^{III} halides.^{17,35} Therefore, we tentatively attribute these low energy absorption bands seen for [Au(L¹)₂Cl₂]Cl **2** and [Au(L²)₂Cl₂]Cl **3** to LMCTs from the chlorido ligands to the Lewis acidic Au^{III} centres. A distinct LMCT band is not seen for [AuL³Cl₂]Cl **4**, but may be overlapped with the high energy absorption band below 300 nm. Similar observations were also reported by Huynh *et al.* for UV-vis studies of [Au^{III}Cl₂(iPr₂Bim)₂]BF₄ (Bim = 1,3-benzimidazol-2-ylidene).³⁵

The molar conductance of solutions of the complexes in DMSO (Table 3) was measured to gain insight into possible dissociation of the chlorido ligands from the Au centres. Solutions of each of the salts [Au(L¹)₂](PF₆)₃ **5**, [Au(L²)₂](PF₆)₃ **6** and [AuL³](PF₆)₃ **7**, showed conductivity in the range 113–119 S cm² mol^{–1}. These values are in the range expected for 1 : 3 electrolytes in DMSO.^{42,43} By contrast, [Au(L¹)₂Cl₂]Cl **2** and [AuL³Cl₂]Cl **4** showed a molar conductivity of 44.5 and 41.8 S cm² mol^{–1} respectively, in the range expected for a 1 : 1 electrolyte, while [Au(L²)₂Cl₂]Cl **3** showed a molar conductivity of 83.5 S cm² mol^{–1}, which falls in the range expected for 1 : 2 electrolytes. These results suggest that for [Au(L¹)₂Cl₂]Cl **2** and [AuL³Cl₂]Cl **4** in DMSO solution, the complex cation is of the form the [Au(NHC)₄Cl₂]⁺ (the same as seen in the solid state), while for [Au(L²)₂Cl₂]Cl **3**, the complex cation is of the form [Au(NHC)₄Cl]²⁺ in DMSO solution. Compared to [Au(L¹)₂Cl₂]⁺ and [AuL³Cl₂]⁺, the higher propensity of [Au(L²)₂Cl₂]⁺ to undergo dissociation of Cl[–] may be consequence of increased steric congestion around the axial coordination sites, as suggested by the steeper inclination of the imidazolyl rings relative to the AuC₄ plane in [Au(L²)₂Cl₂]⁺ (see above).

NMR spectroscopy

The ¹H and ¹³C NMR spectra for Au^{III} tetracarbene complexes (Fig. 5 and S1–S12†) are broadly consistent with the structures



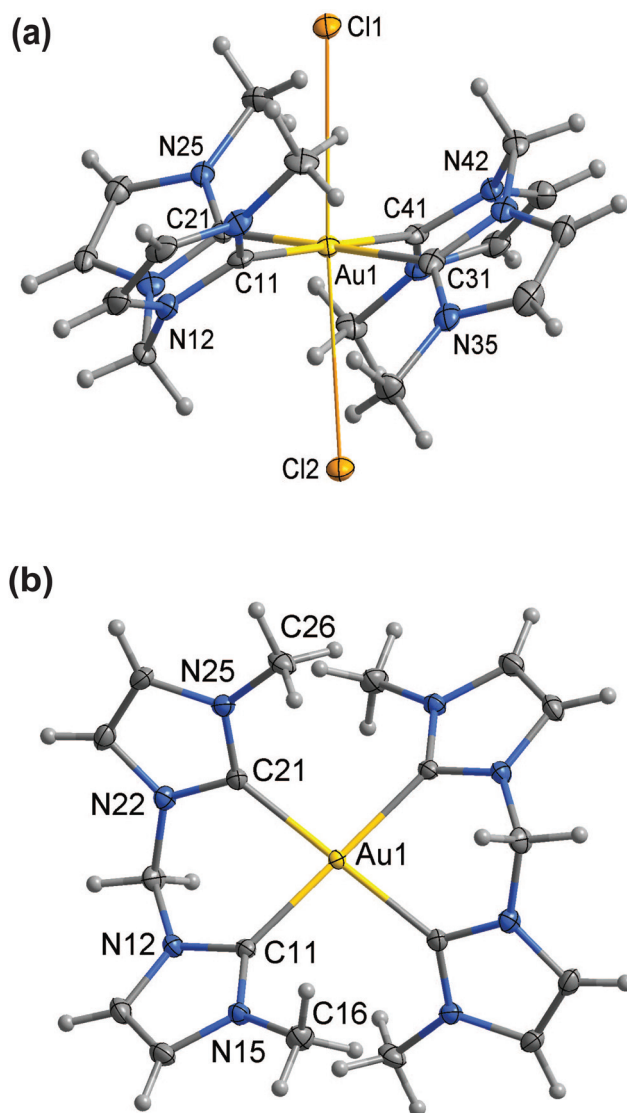


Fig. 1 (a) Crystal structure (50% probability level for the displacement ellipsoids) of the cation of $[\text{Au}(\text{L}^1)_2\text{Cl}_2]\text{Cl}$ **2**. Selected bond lengths (Å) and angles (°): Au(1)–C(11) 2.040(9), Au(1)–C(41) 2.043(9), Au(1)–C(31) 2.046(9), Au(1)–C(21) 2.050(9), Au(1)–Cl(1) 3.148(2), Au(1)–Cl(2) 3.192(2), C(11)–Au(1)–C(41) 179.3(3), C(41)–Au(1)–C(31) 85.0(4), Cl(1)–Au(1)–Cl(2) 176.78(6). (b) Crystal structure (50% probability level for the displacement ellipsoids) of the cation of $[\text{Au}(\text{L}^1)_2](\text{PF}_6)_3$ **5**. PF_6 anions have been omitted for clarity. Selected bond lengths (Å) and angles (°): Au(1)–C(21) 2.041(2), Au(1)–C(11) 2.045(2), C(21)–Au(1)–C(11) 83.31(9).

seen in the solid state, but show effects of dissociation of chlorido in some cases.

The ^1H NMR spectrum of $[\text{Au}(\text{L}^1)_2\text{Cl}_2]\text{Cl}$ **2** in $\text{DMSO}-d_6$ solution shows a single signal due to the methyl protons (3.69 ppm), two doublet signals in the range 7.5–8.5 ppm, corresponding to the two non-equivalent protons of each imidazolyl ring, and a pair of doublets (AX pattern) centred at 8.09 and 6.79 ppm, corresponding to two non-equivalent protons in the methylene bridge linking the imidazolyl groups in each ligand. The non-equivalence of the methylene protons indicates that the “puckered” conformation adopted by the two L^1

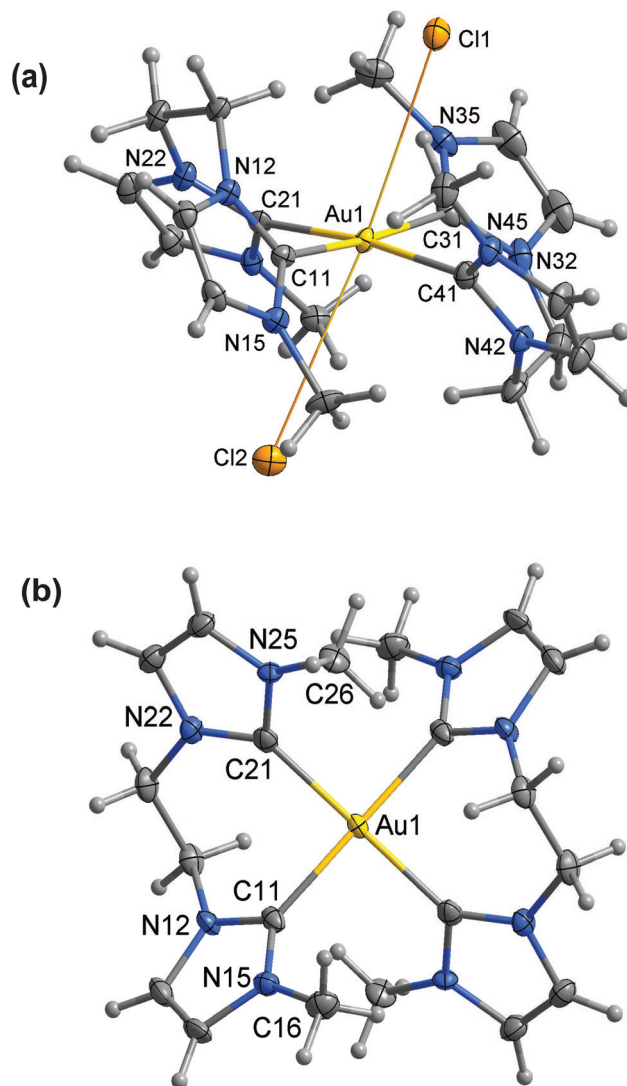


Fig. 2 (a) Crystal structure (50% probability level for the displacement ellipsoids) of the cation of $[\text{Au}(\text{L}^2)_2\text{Cl}_2]\text{Cl}$ **3**. Selected bond lengths (Å) and angles (°): Au(1)–C(11) 2.024(4), Au(1)–C(21) 2.054(4), Au(1)–Cl(1) 3.433(1), Au(1)–Cl(2) 3.693(1), C(11)–Au(1)–C(31) 174.87(17), C(11)–Au(1)–C(21) 89.84(17), Cl(1)–Au(1)–Cl(2) 172.17(3). (b) Crystal structure (50% probability level for the displacement ellipsoids) of the cation of $[\text{Au}(\text{L}^2)_2](\text{PF}_6)_3$ **6**. PF_6 anions have been omitted for clarity. Selected bond lengths (Å) and angles (°): Au(1)–C(11) 2.0402(18), Au(1)–C(21) 2.062(2), C(11)–Au(1)–C(21) 88.22(8).

ligands in the complex in the solid state persists in solution and is rigid on the NMR timescale. The ^1H NMR spectrum of $[\text{Au}(\text{L}^1)_2](\text{PF}_6)_3$ **5** in $\text{DMSO}-d_6$ solution shows the same number of signals and splitting patterns, but the signals are at different chemical shifts, markedly so for the signals of the methylene protons. This observation is consistent with the change in coordination of Au^{III} from $\text{Au}(\text{NHC})_4\text{Cl}_2$ for $[\text{Au}(\text{L}^1)_2\text{Cl}_2]\text{Cl}$ **2** to $\text{Au}(\text{NHC})_4$ for $[\text{Au}(\text{L}^1)_2](\text{PF}_6)_3$ **5**. We tentatively assign the doublet at 8.09 ppm to the *endo* protons of the CH_2 groups, and suggest that its markedly downfield chemical shift is a consequence of an intramolecular $\text{H}\cdots\text{Cl}$ hydrogen bonding interaction with a Cl ligand. Interestingly,



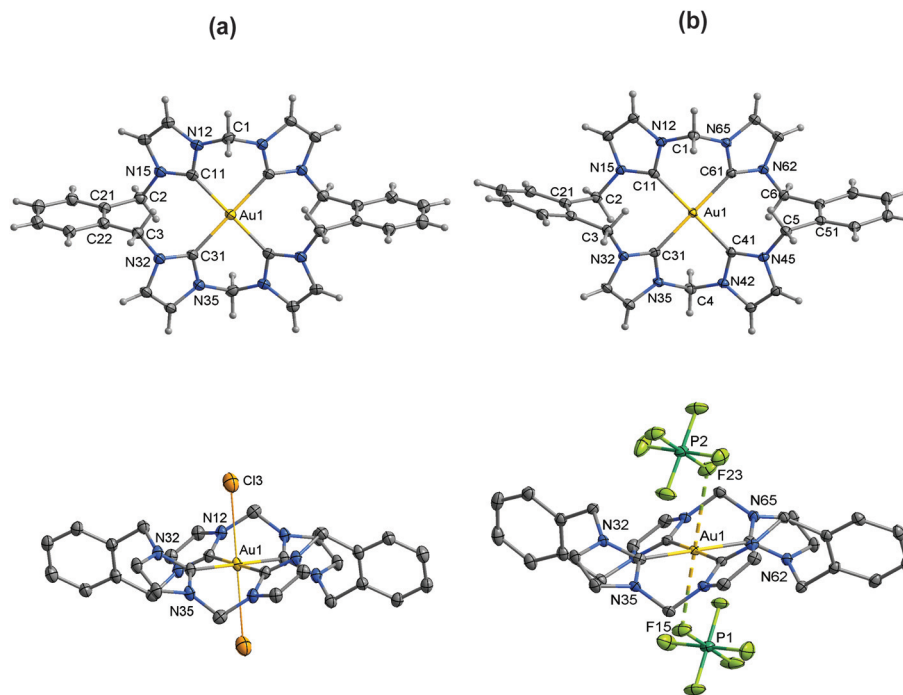


Fig. 3 (a) Crystal structure (30% probability level for the displacement ellipsoids) of the cation of $[\text{AuL}^3\text{Cl}_2]\text{Cl}$ **4**. Selected bond lengths (Å) and angles (°): Au(1)–C(11) 2.048(8), Au(1)–C(31) 2.082(7), Au(1)–Cl(3) 3.017(4), C(11)–Au(1)–C(31) 95.5(3). (b) Crystal structure (50% probability level for the displacement ellipsoids) of the cation 1 of $[\text{AuL}^3](\text{PF}_6)_3$ **7**. (Cation 2 is similar.) Selected bond lengths (Å) and angles (°): Au(1)–C(41) 2.051(2), Au(1)–C(31) 2.052(2), Au(1)–C(11) 2.056(2), Au(1)–C(61) 2.056(2), Au(2)–C(71) 2.050(2), Au(2)–C(91) 2.055(2), Au(1)–F(15) 3.004(5), Au(1)–F(23) 3.089(2), Au(2)–F(33) 3.903(2), C(41)–Au(1)–C(31) 84.77(8), C(41)–Au(1)–C(11) 178.57(8), F(15)–Au(1)–F(23) 179.47(8), C(71)–Au(2)–C(91) 93.94(8).

in the solid state, the $\text{Cl}\cdots\text{H}$ distances for the *endo* hydrogens are 2.55 and 2.60 Å, which are within the range of ~2.2 Å–~3.0 Å seen for $\text{C}\cdots\text{H}\cdots\text{Cl}$ hydrogen bonds.⁴⁴

It is interesting to note that the ^1H NMR chemical shift of the signal for the *endo* CH_2 protons of $[\text{Au}(\text{L}^1)_2\text{Cl}_2]\text{Cl}$ **2** in D_2O solutions is close to that seen for $[\text{Au}(\text{L}^1)_2](\text{PF}_6)_3$ **5** in $\text{DMSO}-d_6$, and markedly different from that seen for $[\text{Au}(\text{L}^1)_2\text{Cl}_2]\text{Cl}$ **2** in $\text{DMSO}-d_6$. This observation suggests in D_2O solution, the cation $[\text{Au}(\text{L}^1)_2\text{Cl}_2]^+$ undergoes solvolysis to give $[\text{Au}(\text{L}^1)_2]^{3+}$. Consistent with this suggestion, we found that when NaCl was dissolved in solutions prepared by dissolving $[\text{Au}(\text{L}^1)_2\text{Cl}_2]\text{Cl}$ **2** in D_2O , the signal for the *endo* CH_2 protons shifted downfield (*i.e.*, towards the chemical shift seen for the *endo* protons in $[\text{Au}(\text{L}^1)_2\text{Cl}_2]^+$), and moved back upfield (*i.e.*, towards the chemical shift seen for the *endo* protons in $[\text{Au}(\text{L}^1)_2]^{3+}$) when Cl^- was precipitated from the sample as AgCl (Fig. S13†).

As noted above, conductance measurements showed that dissolution of $[\text{Au}(\text{L}^2)_2\text{Cl}_2]\text{Cl}$ **3** in DMSO results in dissociation of one Cl^- ligand from the Au centre and formation of $[\text{Au}(\text{L}^2)_2\text{Cl}]^{2+}$ in solution. The ^1H NMR spectra of solutions prepared by dissolving $[\text{Au}(\text{L}^2)_2\text{Cl}_2]\text{Cl}$ **3** in $\text{DMSO}-d_6$ can thus be considered to be spectra of the cation $[\text{Au}(\text{L}^2)_2\text{Cl}]^{2+}$. These spectra again show a single signal (3.35 ppm) due to the methyl protons and two doublet signals (now in the range 7.7–7.9 ppm) corresponding to the two non-equivalent protons of each imidazole ring, with an apparent AA'XX' pattern of signals centred at 4.91 and 5.46 ppm, corresponding to the

protons in each ethylene bridge. These signals and splitting patterns suggest that the “puckered” conformation adopted by the two L^2 ligands of $[\text{Au}(\text{L}^2)_2\text{Cl}_2]^+$ in the solid state persists in solution. In the solid state, there are four non-equivalent environments for the hydrogen atoms in each ethylene bridge, so the observation of an AA'XX' pattern for the ethylene protons suggests that some twisting within each L^2 ligand causes *exo* and *endo* protons on each carbon in an ethylene bridge to be rendered equivalent on the NMR timescale (Fig. 6).

There are small differences between the ^1H NMR signals seen for $[\text{Au}(\text{L}^2)_2\text{Cl}]^{2+}$ and $[\text{Au}(\text{L}^2)_2]^{3+}$ (solutions prepared from $[\text{Au}(\text{L}^2)_2](\text{PF}_6)_3$ **6** in terms chemical shift, but the number of signals and splitting patterns are the same in each case. For $[\text{Au}(\text{L}^2)_2\text{Cl}]^{2+}$, we note that the existence of an $\text{Au}(\text{NHC})_4\text{Cl}$ coordination motif (approximately square pyramidal) must render the two L^2 ligands inequivalent if the ligands are puckered in the same way as seen in the solid state for $[\text{Au}(\text{L}^2)_2\text{Cl}_2]\text{Cl}$ **3**. Since the number of NMR signals is consistent with the L^2 ligands being equivalent on the NMR timescale, it may be that the two L^2 ligands are rendered equivalent on the NMR timescale by rapid dissociation and re-association of the chlorido ligand (Fig. 5(b)).

The ^1H NMR spectra for both $[\text{AuL}^3\text{Cl}_2]\text{Cl}$ **4** and $[\text{AuL}^3](\text{PF}_6)_3$ **7** in $\text{DMSO}-d_6$ solution are analogous to those seen for $[\text{Au}(\text{L}^1)_2\text{Cl}_2]\text{Cl}$ **2** and $[\text{Au}(\text{L}^1)_2](\text{PF}_6)_3$ **5**. Major differences between the two samples in terms of in chemical shifts of the



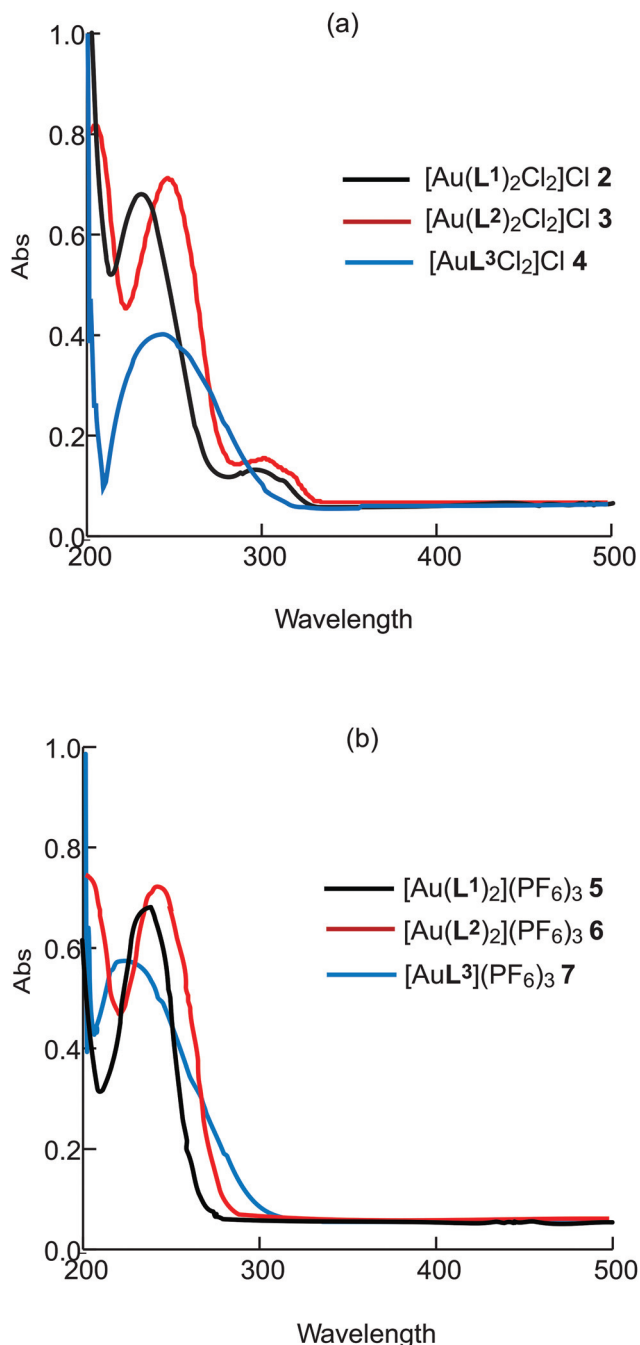


Fig. 4 UV-vis absorption spectra of (a) $[\text{Au}(\text{L}^1)_2\text{Cl}_2]\text{Cl}$ 2, $[\text{Au}(\text{L}^2)_2\text{Cl}_2]\text{Cl}$ 3, $[\text{AuL}^3\text{Cl}_2]\text{Cl}$ 4 and (b) $[\text{Au}(\text{L}^1)_2](\text{PF}_6)_3$ 5, $[\text{Au}(\text{L}^2)_2](\text{PF}_6)_3$ 6, $[\text{AuL}^3](\text{PF}_6)_3$ 7 in MeCN.

protons of the methylene linkers, and to a lesser extent those of the benzylic protons, are consistent with a change in coordination of Au^{III} , from $\text{Au}(\text{NHC})_4\text{Cl}_2$ in $[\text{AuL}^3\text{Cl}_2]\text{Cl}$ 4 to $\text{Au}(\text{NHC})_4$ (or a solvated form) in $[\text{AuL}^3](\text{PF}_6)_3$ 7. The number of signals and splitting patterns are consistent with the ligand L^3 adopting a “puckered” conformation that does not invert on the NMR timescale.

In the ^{13}C NMR spectra of the new Au^{III} -NHC complexes having an $\text{Au}(\text{NHC})_4$ motif, the signal for the carbene carbon

Table 3 UV-vis spectroscopic data and conductivity properties of Au^{III} -NHC complexes

Complex	$\lambda_{\text{max}}/\text{nm}$ ($\epsilon/\text{M}^{-1}\text{cm}^{-1}$) ^a	Λ_{M} ^b ($\text{S cm}^2\text{mol}^{-1}$)
$[\text{Au}(\text{L}^1)_2\text{Cl}_2]\text{Cl}$ 2	302 (3600), 235 (14 100)	41.6
$[\text{Au}(\text{L}^1)_2](\text{PF}_6)_3$ 5	250 (14 600)	114.6
$[\text{Au}(\text{L}^2)_2\text{Cl}_2]\text{Cl}$ 3	301 (4100), 245 (15 200)	83.5
$[\text{Au}(\text{L}^2)_2](\text{PF}_6)_3$ 6	241 (15 000)	118.7
$[\text{AuL}^3\text{Cl}_2]\text{Cl}$ 4	275 (8400)	41.8
$[\text{AuL}^3](\text{PF}_6)_3$ 7	256 (11 600)	113.4

^a Measured in 0.05 mM MeCN solution at 298 K. ^b Measured in 1 mM DMSO solution at 298 K.

occurs near 146 ppm, which is close to that reported for the related $[\text{Au}(\text{NHC})_4]^+$ complex **1**³² but approximately 35 ppm upfield of that for the carbene carbons in Au^{I} -NHC complexes.⁸ For comparison, imidazolium-derived Au^{III} complexes of form $[\text{Au}(\text{R}_2\text{Im})\text{Cl}_3]$ (R_2Im = 1,3-dialkylimidazol-2-ylidene) show a carbene signal in the range 134–141 ppm,^{14,45} and $[\text{Au}(\text{R}_2\text{Im})_2\text{Cl}_2]^+$ and $[\text{Au}_2(\text{L}^1)_2\text{Cl}_4]^{2+}$ exhibit carbene signals near 150–155 ppm,^{46,47} while $[\text{Au}(\text{R}_2\text{Bim})\text{Cl}_3]$ and $[\text{Au}(\text{R}_2\text{Bim})_2\text{Cl}_2]^+$ (R_2Bim = 1,3-dialkylbenzimidazol-2-ylidene) exhibit carbene signals³⁵ about 10 ppm downfield of those of their imidazolium-derived counterparts.

H-D exchange reactions

Imidazolium ions are well-known to undergo H/D exchange reactions.^{48–50} We have explored H/D exchange reactions for the imidazolium salt $\text{L}^1\cdot 2\text{HCl}$ and the Au^{III} complex $[\text{Au}(\text{L}^1)_2]^{3+}$ (formed from $[\text{Au}(\text{L}^1)_2\text{Cl}_2]\text{Cl}$ 2, see above) in D_2O solutions (Fig. 7). For $\text{L}^1\cdot 2\text{HCl}$, the imidazolium H2 protons exchange quickly (<5 min at room temperature) with deuterium from the solvent. This finding is consistent with previous observations that the ^1H NMR signal for the H2 protons of imidazolium salts generally “underintegrates” in spectra recorded in D_2O and methanol- d_4 solutions at room temperature.^{51–53} When the sample was heated at 100 °C, the imidazolyl H4/H5 protons were fully exchanged over the course of about 48 h, while the CH_2 protons were about 40% exchanged over the same period, and the CH_3 protons underwent little or no exchange. The analogous exchange reactions were markedly faster for $[\text{Au}(\text{L}^1)_2]^{3+}$ under similar conditions: the imidazolyl H4/H5 protons (δ 7.91, 7.61 ppm) were fully exchanged within 17 h at 100 °C, as indicated by disappearance of the H4/H5 signals from the ^1H NMR spectrum, and the CH_2 protons were fully exchanged within 48 h at 100 °C (Fig. 7b). Experiments conducted using *t*-butanol as an internal standard showed negligible H/D exchange of CH_3 protons in $[\text{Au}(\text{L}^1)_2]^{3+}$ even after heating for 48 h (Fig. S14†). Not surprisingly, the H/D exchange reactions of $[\text{Au}(\text{L}^1)_2]^{3+}$ were catalysed by base—in the presence of two equivalents of K_2CO_3 , the imidazolyl H4/H5 protons (but not the CH_2 protons) underwent partial exchange over 48 h at room temperature (Fig. S15†), and in the presence of two equivalents of NaOH, both the imidazolyl H4/H5 protons and the CH_2 protons were almost completely exchanged overnight at room temperature (Fig. S16†). The



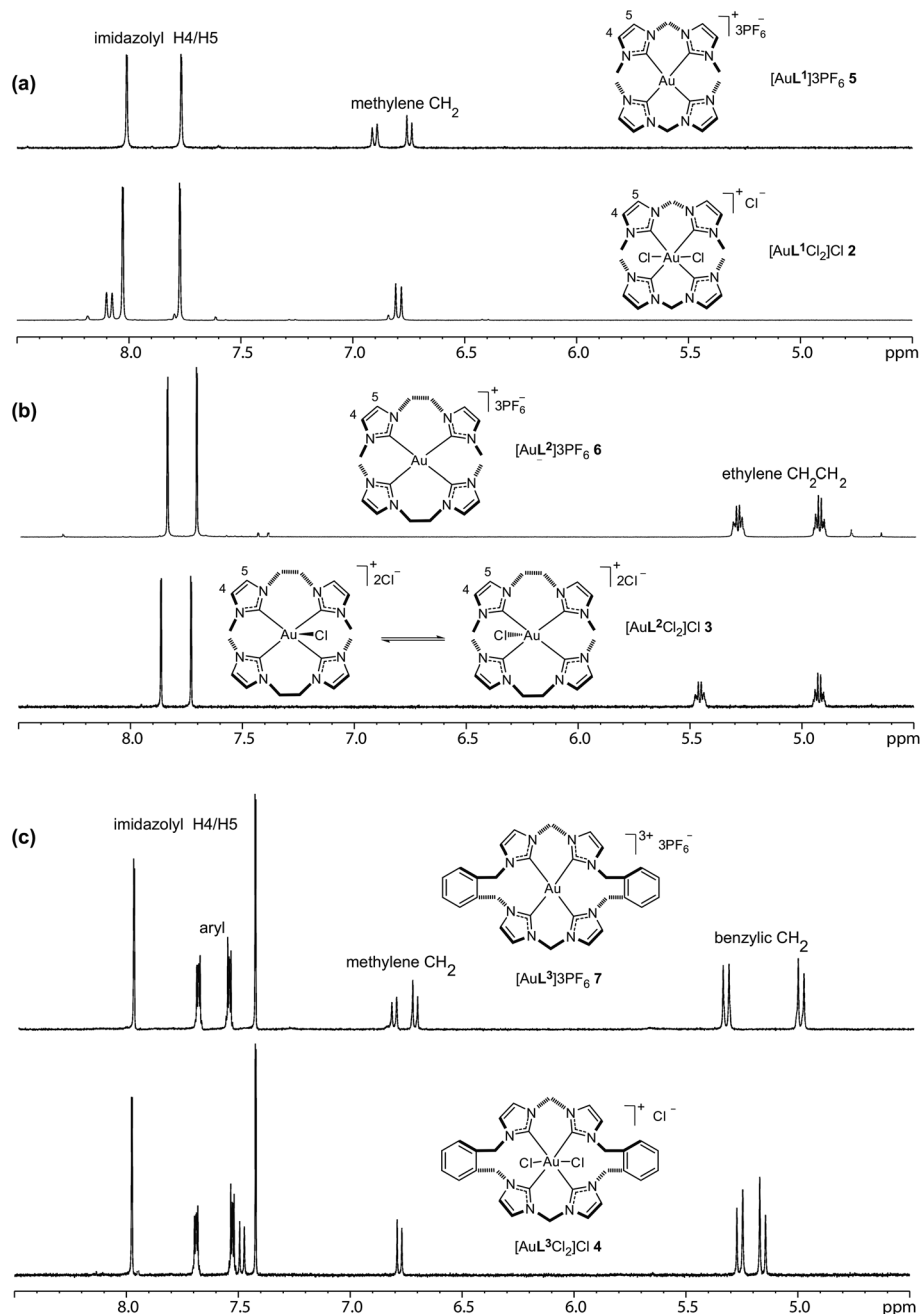


Fig. 5 ^1H NMR spectra (600 MHz, $\text{DMSO}-d_6$) for: (a) $[\text{Au}(\text{L}^1)_2\text{Cl}]\text{Cl}$ **2**, $[\text{Au}(\text{L}^1)_2](\text{PF}_6)_3$ **5**; (b) $[\text{Au}(\text{L}^2)_2\text{Cl}]\text{Cl}$ **3**, $[\text{Au}(\text{L}^2)_2](\text{PF}_6)_3$ **6**; and (c) $[\text{Au}(\text{L}^3)_2\text{Cl}]\text{Cl}$ **4**, $[\text{Au}(\text{L}^3)_2](\text{PF}_6)_3$ **7**.

high charge on the $[\text{Au}(\text{L}^1)_2]^{3+}$ cation is likely a factor contributing to the fast H/D exchange seen in D_2O (formation of a deprotonated intermediate $[\text{Au}(\text{L}^1)_2\text{H}]^{2+}$ would be favoured by the concomitant decrease in concentration of positive charge on the complex).

Stability studies

The new $\text{Au}^{\text{III}}(\text{NHC})_4$ complexes reported in this work were stable in the solid state at room temperature under air for at least 1 year. The D_2O exchange experiment described above

suggests surprisingly high stability for the $\text{Au}^{\text{III}}(\text{NHC})_4$ complexes, in that they can survive extended periods in solution at 100°C , albeit with H/D exchange occurring. To further explore the stability of the new $\text{Au}^{\text{III}}(\text{NHC})_4$ complexes, we have used ^1H NMR spectroscopy to assess the longevity of various samples in $\text{DMSO}-d_6$ solutions at elevated temperatures. After a $\text{DMSO}-d_6$ solution containing $[\text{Au}(\text{L}^1)_2](\text{PF}_6)_3$ **5** was stored at room temperature for 6 months and then heated at 120°C for 26 h, there was no significant change to the ^1H NMR spectrum (Fig. S17 †). The same applied for a $\text{DMSO}-d_6$ solution contain-



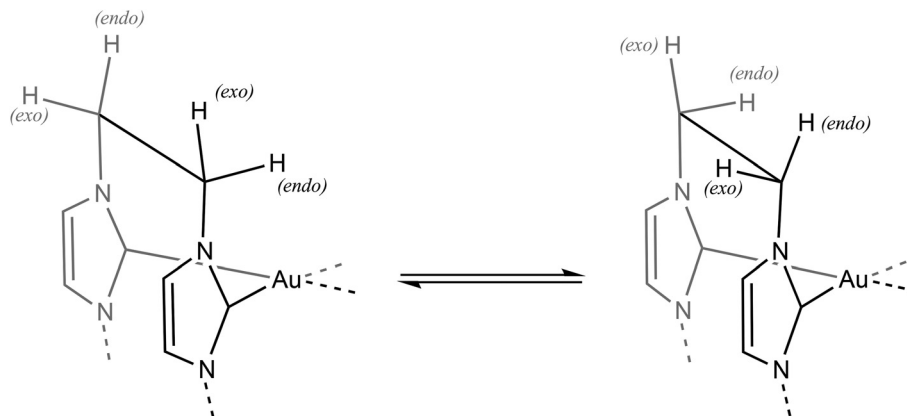


Fig. 6 Proposed twisting of the ethylene bridge to account for symmetry observed for ^1H NMR signals of $[\text{Au}(\text{L}^2)_2\text{Cl}_2]\text{Cl}$ **3** in $\text{DMSO}-d_6$ solution.

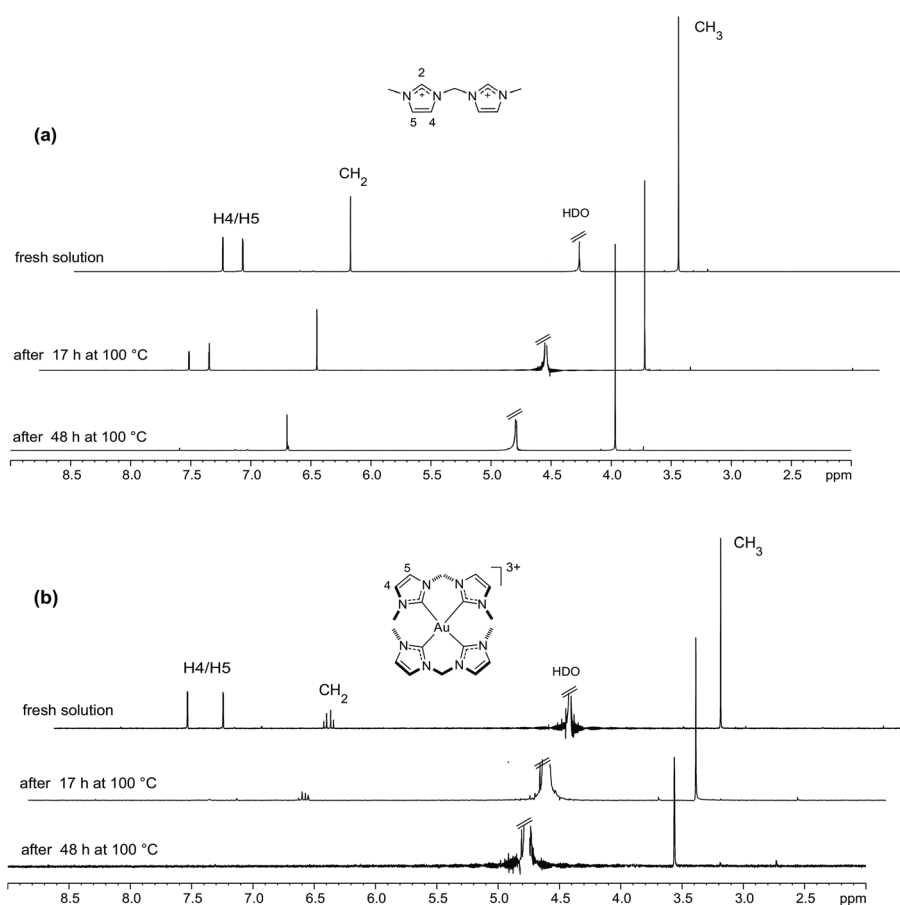


Fig. 7 ^1H NMR spectra (600.13 MHz, D_2O) for solutions of (a) the imidazolium salt $\text{L}^1\cdot 2\text{HCl}$ and (b) the Au^{III} complex $[\text{Au}(\text{L}^1)_2]^{3+}$ (prepared from $[\text{Au}(\text{L}^1)_2\text{Cl}_2]\text{Cl}$ **2**), showing disappearance of signals due to H/D exchange reactions. For $\text{L}^1\cdot 2\text{HCl}$, no signal for the H2 protons was detected even from freshly-prepared solutions.

ing $[\text{Au}(\text{L}^3)](\text{PF}_6)_3$ **7** that was maintained at 120°C for 7 days (Fig. S19†). The chlorido complex $[\text{Au}(\text{L}^2)_2\text{Cl}_2]\text{Cl}$ **3** was somewhat less stable; after a $\text{DMSO}-d_6$ solution containing this compound was heated at 120°C for 7 days, integration of the imidazolyl H4/H5 region of the ^1H NMR spectrum indicating that ca. 20% of the initial Au^{III} complex $[\text{Au}(\text{L}^2)_2\text{Cl}_2]^+$ had

decomposed, the major decomposition product being the known⁵⁴ dinuclear Au^{I} complex $[\text{Au}_2(\text{L}^2)_2]^{2+}$ (Fig. S18†). The slightly lower stability of $[\text{Au}(\text{L}^2)_2\text{Cl}_2]^+$ may be a consequence of slightly higher strain in the chelate rings (e.g., in the ethylene link joining the NHC units in $[\text{Au}(\text{L}^2)_2\text{Cl}_2]^+$, N–C–C angles are $113.4(3)$, $113.8(4)$, $115.7(4)$ and $116.4(4)^\circ$; in the methylene



linker in $[\text{Au}(\text{L}^1)_2\text{Cl}_2]^+$, N–C–N angles are 108.5(7) and 109.1(7)°, closer to the ideal tetrahedral angle, 109.5°. For comparison, salts of the dinuclear Au^{III} complex $[\text{Au}_2(\text{L}^1)_2\text{Cl}_4]^{2+}$ and its bromido counterpart,^{8,47} which contain $\text{Au}^{\text{III}}(\text{NHC})_2\text{X}_2$ moieties rather than $\text{Au}^{\text{III}}(\text{NHC})_4$ moieties, were far less stable. At room temperature in the solid state, *ca.* 50% of the $\text{Au}^{\text{III}}/\text{Au}^{\text{III}}$ complex $[\text{Au}_2(\text{L}^1)_2\text{Br}_4]^{2+}$ had decomposed to the $\text{Au}^{\text{I}}/\text{Au}^{\text{III}}$ complex $[\text{Au}_2(\text{L}^1)_2\text{Br}_2]^{2+}$ over 6 months (Fig. S20 and S21†), and no Au^{III} species could be detected after a DMSO-*d*₆ solution containing $[\text{Au}_2(\text{L}^1)_2\text{Br}_4]^{2+}$ and $[\text{Au}_2(\text{L}^1)_2\text{Br}_2]^{2+}$ was heated at 120 °C for 2 h (Fig. S21†). Similar results were seen for solutions containing $[\text{Au}_2(\text{L}^1)_2\text{Cl}_4]^{2+}$ (Fig. S22†) and $[\text{Au}_2(\text{L}^2)_2\text{Br}_4]^{2+}$ (Fig. S23†).

The high stability of $\text{Au}^{\text{III}}(\text{NHC})_4$ complexes compared to their $\text{Au}^{\text{III}}(\text{NHC})_2(\text{halide})_2$ counterparts may reflect the strong σ -donating ability of the NHC ligand, which is better able to stabilise the Au^{III} centre than the weaker σ -donating halide ligands. The robustness of the metal–NHC bond and steric protection exerted by the chelating NHC ligands must also contribute to the enhanced stability of the $\text{Au}^{\text{III}}(\text{NHC})_4$ complexes compared to their $\text{Au}^{\text{III}}(\text{NHC})_2\text{X}_2$ counterparts.

Cyclovoltammetric studies showed that the Au^{III} complexes did not undergo reversible redox reactions at room temperature in acetonitrile with Bu_4NClO_4 as electrolyte (see ESI†).

Conclusion

Three new Au^{III} complexes of form $[\text{Au}(\text{NHC})_4\text{Cl}_2]\text{Cl}$ may be synthesized in good yield directly from bis- and tetrakis(imidazolium) salts and KAuCl_4 in the presence of base. These formally 20 electron complexes have tetragonally distorted octahedral coordination of the Au^{III} centre, the NHC groups making an approximately square planar array and the chlorido ligands occupying more distant axial positions. The $\text{Au}^{\text{III}}(\text{NHC})_4$ motif is remarkably stable, resisting decomposition in DMSO solution at 120 °C or D_2O at 100 °C for extended periods. The axial (chlorido) ligands are labile, and metathesis of the $[\text{Au}(\text{NHC})_4\text{Cl}_2]\text{Cl}$ salts with KPF_6 in methanol/water results in removal of the chlorido ligands and formation of three new, formally 16 electron complexes of form $[\text{Au}(\text{NHC})_4](\text{PF}_6)_3$. The $[\text{Au}(\text{NHC})_4]^{3+}$ ion is sufficiently stable to undergo base-catalysed H/D exchange reactions at most sites on the NHC ligands in D_2O at 100 °C without evidence of decomposition.

Experimental section

General procedures

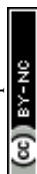
Nuclear magnetic resonance spectra were recorded using Bruker ARX400 (400.13 MHz for ^1H), Bruker ARX500 (500.13 MHz for ^1H and 125.77 MHz for ^{13}C), or Bruker ARX 600 (600.13 MHz for ^1H , 150.90 MHz for ^{13}C) spectrometers at ambient temperature. ^1H and ^{13}C NMR chemical shifts were referenced to signals of the solvent (DMSO-*d*₆: ^1H 2.50 ppm;

^{13}C 39.52). When necessary, assignments were made with the aid of ^1H – ^{13}C HSQC (heteronuclear single quantum coherence) and ^1H – ^{13}C HMBC (heteronuclear multiple bond correlation) spectra. Conductance measurements were performed by using a TPS Aqua-CP/A conductivity meter. Cyclic voltammetry experiments were recorded using an eDAQ e-corder 401 system in a three-electrode cell with a glassy carbon (1 mm diameter) working electrode, a platinum (1 mm diameter) counter electrode, and a platinum wire reference electrode. Measurements were taken at room temperature (25 °C) in acetonitrile with 0.1 M Bu_4NClO_4 as a supporting electrolyte. Microanalyses were performed by The School of Chemistry & Molecular Bioscience, University of Queensland, Australia, and the Instrument Center of National Chung Hsing University, Taiwan. High resolution mass spectra were measured using Agilent LCMS 6510 Q-TOF and Waters LCT Premier XE spectrometers, using the ESI method, with $\text{MeCN}:\text{H}_2\text{O}$ (9:1) as solvent. All organometallic compounds were prepared under a nitrogen atmosphere. The imidazolium salts $\text{L}^1\cdot 2\text{HCl}$, $\text{L}^2\cdot 2\text{HCl}$,^{55,56} and $\text{L}^3\cdot 4\text{HCl}$ ⁵⁷ were prepared according to literature procedures, and the Au^{III} complexes $[\text{Au}_2(\text{L}^1)_2\text{X}_4]\text{X}_2$ (X = Cl, Br) and $[\text{Au}_2(\text{L}^2)_2\text{Br}_4]\text{Br}_2$ were prepared in the same way as the corresponding hexafluorophosphate salts.^{8,47}

Synthesis of Au^{III} –NHC complexes

Complex 2, $[\text{Au}(\text{L}^1)_2\text{Cl}_2]\text{Cl}$. A solution of LiOAc (80 mg, 1.21 mmol) in DMF (5 mL) was added to a solution of the bis(imidazolium) salt $\text{L}^1\cdot 2\text{HCl}$ (99 mg, 0.40 mmol) and KAuCl_4 (75 mg, 0.20 mmol) in DMF (10 mL) at 80 °C. The mixture was then heated to 100 °C and maintained at that temperature for 5 h. During this time a white precipitate formed. The precipitate was collected by filtration and washed successively with DMF, acetone, and Et_2O to give $[\text{Au}(\text{L}^1)_2\text{Cl}_2]\text{Cl}$ 2 as a white powder (106 mg, 81%). Found: C, 32.88; H, 3.66; N, 17.10%. $\text{AuC}_{18}\text{H}_{24}\text{N}_8\text{Cl}_3$ requires C, 32.97; H, 3.69; N, 17.09%. ^1H NMR (600.13 MHz, DMSO-*d*₆): δ 8.09 (d, $^2J_{\text{H,H}}$ 15.3 Hz, 2H, CHH), 8.03 (d, $^3J_{\text{H,H}}$ 2.1 Hz, 4H, imidazolyl H4/H5), 7.77 (d, $^3J_{\text{H,H}}$ 2.1 Hz, 4H, imidazolyl H4/H5), 6.79 (d, $^2J_{\text{H,H}}$ 15.3 Hz, 2H, CHH), 3.69 (s, 12H, 4 × CH₃). $^{13}\text{C}\{^1\text{H}\}$ NMR (150.9 MHz, DMSO-*d*₆): δ 146.82 (NCN), 124.96 (imidazolyl C4/C5), 123.63 (imidazolyl C4/C5), 63.15 (CH₂), 37.78 (CH₃). HRMS (ESI⁺): calcd for $\text{AuC}_{18}\text{H}_{24}\text{N}_8\text{Cl}_2^+$ ($[\text{AuL}^1\text{Cl}_2]^+$), *m/z* 619.1166. Found, *m/z* 619.1160.

Complex 5, $[\text{Au}(\text{L}^1)_2](\text{PF}_6)_3$. A solution of KPF_6 (106 mg, 0.58 mmol) in water (3 mL) was added to a solution of $[\text{Au}(\text{L}^1)_2\text{Cl}_2]\text{Cl}$ 2 (106 mg, 0.17 mmol) in MeOH (10 mL). The resulting precipitate was collected by filtration and washed with water and (3 × 3 mL) with methanol to leave $[\text{Au}(\text{L}^1)_2](\text{PF}_6)_3$ 5 as a white powder (93 mg, 59%). Found: C, 21.88; H, 2.57; N, 11.43%. $\text{AuC}_{18}\text{H}_{24}\text{N}_8\text{P}_3\text{F}_{18}$ requires C, 21.96; H, 2.46; N, 11.38%. ^1H NMR (600.13 MHz, DMSO-*d*₆): δ 8.01 (d, $^3J_{\text{H,H}}$ 1.8 Hz, 4H, imidazolyl H4/H5), 7.77 (d, $^3J_{\text{H,H}}$ 1.8 Hz, 4H, imidazolyl H4/H5), 6.84 (d, $^2J_{\text{H,H}}$ 13.2 Hz, 2H, CHH), 6.75 (d, $^2J_{\text{H,H}}$ 13.2 Hz, 2H, CHH), 3.50 (s, 12H, 4 × CH₃). $^{13}\text{C}\{^1\text{H}\}$ NMR (150.9 MHz, DMSO-*d*₆): δ 146.68 (NCN), 125.16 (imidazolyl C4/C5), 124.28 (imidazolyl C4/C5), 63.09 (CH₂), 37.83 (CH₃).



HRMS (ESI⁺): calcd for AuC₁₈H₂₄N₈P₂F₁₂⁺ ([Au(L¹)₂·2PF₆]⁺), *m/z* 839.1073. Found: *m/z* 839.1071.

Complex 3, [Au(L²)₂Cl₂]Cl. A solution of LiOAc (61 mg, 0.92 mmol) in DMF (5 mL) was added to a solution of the bis(imidazolium) salt L²·2HCl (105 mg, 0.40 mmol) and KAuC₄ (75 mg, 0.20 mmol) in DMF (10 mL) at 80 °C. The mixture was then heated to 110 °C and maintained at that temperature overnight. The white precipitate that formed was collected by filtration and washed successively with DMF, acetone, and Et₂O, to leave [Au(L²)₂Cl₂]Cl **3** as a white powder (108 mg, 79%). Found: C, 35.32; H, 4.33; N, 16.05% AuC₂₀H₂₈N₈Cl₃ requires C, 35.13; H, 4.13; N, 16.39%. ¹H NMR (600.13 MHz, DMSO-*d*₆): δ 7.86 (d, ³*J*_{H,H} 2.1 Hz, 4H, imidazolyl H4/H5), 7.73 (d, ³*J*_{H,H} 2.1 Hz, 4H, imidazolyl H4/H5), 5.46 (m, 4H, CH₂CH₂), 4.91 (m, 4H, CH₂CH₂), 3.35 (s, 12H, 4 × CH₃). ¹³C{¹H} NMR (150.9 MHz, DMSO-*d*₆): δ 144.58 (NCN), 126.47 (imidazolyl C4/C5), 125.13 (imidazolyl C4/C5), 47.64 (CH₂CH₂), 38.01 (CH₃). HRMS (ESI⁺): calcd for AuC₂₀H₂₈N₈Cl₂⁺ ([Au(L²)₂Cl₂]⁺) *m/z* 647.1479. Found, *m/z* 647.1464.

Complex 6, [Au(L²)₂](PF₆)₃. This compound was prepared in the same way as [Au(L¹)₂](PF₆)₃ **5**, and was obtained in 69% yield. Found: C, 23.13; H, 3.30; N, 10.80% AuC₂₀H₂₈N₈P₃F₁₈·(H₂O) requires C, 23.31; H, 2.93; N, 10.88%. ¹H NMR (600.13 MHz, DMSO-*d*₆): δ 7.84 (d, ³*J*_{H,H} 1.8 Hz, 4H, imidazolyl H4/H5), 7.71 (d, ³*J*_{H,H} 1.8 Hz, 4H, imidazolyl H4/H5), 5.30 (m, 4H, CH₂CH₂), 4.93 (m, 4H, CH₂CH₂), 3.30 (s, 12H, 4 × CH₃). ¹³C{¹H} NMR (150.9 MHz, DMSO-*d*₆): δ 145.14 (NCN), 127.05 (imidazolyl C4/C5), 125.76 (imidazolyl C4/C5), 47.92 (CH₂CH₂), 38.19 (CH₃). HRMS (ESI⁺): calcd for AuC₂₀H₂₈N₈P₂F₁₂⁺ ([Au(L²)₂·2PF₆]⁺) *m/z* 867.1386. Found, *m/z* 867.1344.

Complex 4, [AuL³Cl₂]Cl. A solution of LiOAc (20 mg, 0.30 mmol) in DMF (5 mL) added to a solution of the tetra(imidazolium) salt L³·4HCl (54 mg, 0.083 mmol) and KAuC₄ (32 mg, 0.083 mmol) in DMF (10 mL) at 80 °C and this temperature was maintained for overnight. The white precipitate that formed was collected by filtration and washed successively with DMF, acetone, and Et₂O to leave [AuL³Cl₂]Cl **4** as a white powder (32 mg, 48%). Found: C, 44.65; H, 3.52; N, 13.83% AuC₃₀H₂₈N₈Cl₃ requires C, 44.82; H, 3.51; N, 13.94%. ¹H NMR (600.13 MHz, DMSO-*d*₆): δ 7.97 (d, ³*J*_{H,H} 2.1 Hz, 4H, imidazolyl H4/H5), 7.68, 7.52 (m, 8H, C₆H₄), 7.48 (d, ²*J*_{H,H} 12.6 Hz, 2H, CHH), 7.42 (d, ³*J*_{H,H} 2.1 Hz, 4H, imidazolyl H4/H5), 6.78 (d, ²*J*_{H,H} 12.6 Hz, 2H, CHH), 5.26 (d, ²*J*_{H,H} 15.6 Hz, 4H, benzylic CHH), 5.15 (d, ²*J*_{H,H} 15.6 Hz, 4H, benzylic, CHH). ¹³C{¹H} NMR (150.9 MHz, DMSO-*d*₆): δ 145.92 (NCN), 134.96 (C₆H₄), 132.20 (C₆H₄), 129.70 (C₆H₄), 125.11 (imidazolyl C4/C5), 123.73 (imidazolyl C4/C5), 62.20 (CH₂), 52.64 (benzylic CH₂). HRMS (ESI⁺): calcd for AuC₃₀H₂₈N₈Cl₂⁺ ([AuL³Cl₂]⁺) *m/z* 767.1479. Found, *m/z* 767.1469.

Complex 7, [AuL³](PF₆)₃. This compound was prepared in the same way as [Au(L¹)₂](PF₆)₃ **5**, and was obtained in 72% yield. Found: C, 31.90; H, 2.39; N, 9.73% AuC₃₀H₂₈N₈P₃F₁₈ requires C, 31.82; H, 2.49; N, 9.89%. ¹H NMR (600.13 MHz, DMSO-*d*₆): δ 7.98 (d, ³*J*_{H,H} 1.8 Hz, 4H, imidazolyl H4/H5), 7.69, 7.56 (m, 8H, C₆H₄), 7.44 (d, ³*J*_{H,H} 1.8 Hz, 4H, imidazolyl H4/H5), 6.82 (d, ²*J*_{H,H} 13.2

Hz, 2H, CHH), 6.72 (d, ²*J*_{H,H} 13.2 Hz, 2H, CHH), 5.34 (d, ²*J*_{H,H} 15.3 Hz, 4H, benzylic CHH), 5.00 (d, ²*J*_{H,H} 15.3 Hz, 4H, benzylic CHH). ¹³C{¹H} NMR (150.9 MHz, DMSO-*d*₆): δ 146.21 (NCN), 134.86 (C₆H₄), 132.20 (C₆H₄), 129.86 (C₆H₄), 125.86 (imidazolyl C4/C5), 124.21 (imidazolyl C4/C5), 62.24 (CH₂), 52.32 (benzylic CH₂). HRMS (ESI⁺): calcd for AuC₃₀H₂₈N₈P₂F₁₂⁺ ([AuL³·2PF₆]⁺) *m/z* 987.1386. Found, *m/z* 987.1396.

X-Ray crystal structure determinations

Crystals of [Au(L¹)₂](PF₆)₃·(MeCN)₂ **5**·(MeCN)₂, [Au(L²)₂](PF₆)₃·(MeCN)₂ **6**·(MeCN)₂ and [AuL³](PF₆)₃·(MeCN)₃ **7**·(MeCN)₃ were grown by diffusion of vapours between neat diethyl ether and a solution of the complex in acetonitrile, and crystals of [Au(L¹)₂Cl₂]Cl·(MeOH)₂ **2**·(MeOH)₂, [Au(L²)₂Cl₂]Cl·(MeOH) **3**·(MeOH) and [AuL³Cl₂]Cl·(MeOH)_{3.5} **4**·(MeOH)_{3.5} were grown by diffusion of vapours between neat diethyl ether and a solution of the complex in methanol. Crystallographic data were collected at 100(2) K on either an Oxford Diffraction Gemini or an Oxford Diffraction Xcalibur diffractometer using Mo Kα or Cu Kα radiation. Following analytical absorption corrections and solution by direct methods, the structures were refined against *F*² with full-matrix least-squares using the program SHELXL-2014.⁵⁸ Unless stated differently below, all hydrogen atoms were added at calculated positions and refined by use of riding models with isotropic displacement parameters based on those of the parent atoms. Except for those atoms mentioned below, anisotropic displacement parameters were employed throughout for the non-hydrogen atoms. For the structure of [AuL³Cl₂]Cl·(MeOH)_{3.5} **4**·(MeOH)_{3.5}, one chlorido ligand was modelled as being disordered with a molecule of methanol with site occupancies constrained to 0.75 and 0.25 from trial refinement and as required for charge balance. Remaining solvent molecules were modelled as three molecules of methanol situated on a crystallographic mirror plane. Geometries and displacement parameters of the solvent were restrained to reasonable values. Solvent hydrogen atoms were not included in the model. For the structure of [Au(L¹)₂](PF₆)₃·(MeCN)₂ **5**·(MeCN)₂, the solvent acetonitrile molecule was found to be disordered over two sites with the methyl atom common to both components. In [Au(L²)₂](PF₆)₃·(MeCN)₂ **6**·(MeCN)₂, the ligand and one hexafluorophosphate anion are both disordered over two sets of sites with occupancies refined to 0.765(4) and its complement after trial refinement showed no significant differences in the refined values. The atoms of the minor component of the cation were refined with isotropic displacement parameters. The remaining hexafluorophosphate anion was modelled as being rotationally disordered with site occupancies were constrained to 0.5 after trial refinement. The solvent was modelled as acetonitrile, disordered over two sets of sites. For the structure of [AuL³](PF₆)₃·(MeCN)₃ **7**·(MeCN)₃, the fluorine atoms of two hexafluorophosphate anions were modelled as being disordered over two sites; hexafluorophosphate anion (1) where site occupancies were refined to 0.75(2) and its complement and hexafluorophosphate anion (3) where fluorine occupancies were constrained to 0.5 after trial refinement.



Acknowledgements

The authors acknowledge the facilities, and the scientific and technical assistance of the Australian Microscopy & Microanalysis Research Facility at the Centre for Microscopy, Characterisation & Analysis, The University of Western Australia. Ahmed H. Mageed thanks The Higher Committee for Education Development in Iraq (HCED) for financial support.

References

- 1 P. J. Barnard, M. V. Baker, S. J. Berners-Price, B. W. Skelton and A. H. White, *Dalton Trans.*, 2004, 1038–1047.
- 2 M. P. Rigobello, A. Folda, B. Dani, R. Menabò, G. Scutari and A. Bindoli, *Eur. J. Pharmacol.*, 2008, **582**, 26–34.
- 3 W. Liu and R. Gust, *Chem. Soc. Rev.*, 2013, **42**, 755–773.
- 4 D. Pflästerer and A. S. K. Hashmi, *Chem. Soc. Rev.*, 2016, **45**, 1331–1367.
- 5 H. Schmidbaur and A. Schier, in *Comprehensive Organometallic Chemistry III*, ed. R. H. Crabtree and D. M. P. Mingos, Elsevier, Oxford UK, 2007, vol. 2, pp. 252–308.
- 6 T. Zou, C. T. Lum, C.-N. Lok, J.-J. Zhang and C.-M. Che, *Chem. Soc. Rev.*, 2015, **44**, 8786–8801.
- 7 I. J. Lin and C. S. Vasam, *Can. J. Chem.*, 2005, **83**, 812–825.
- 8 M. Baron, C. Tubaro, M. Basato, A. Biffis, M. M. Natile and C. Graiff, *Organometallics*, 2011, **30**, 4607–4615.
- 9 P. de Frémont, R. Singh, E. D. Stevens, J. L. Petersen and S. P. Nolan, *Organometallics*, 2007, **26**, 1376–1385.
- 10 S. Zhu, R. Liang and H. Jiang, *Tetrahedron*, 2012, **68**, 7949–7955.
- 11 I. G. Santos, A. Hagenbach and U. Abram, *Dalton Trans.*, 2004, 677–682.
- 12 S. D. Khanye, N. B. Báthori, G. S. Smith and K. Chibale, *Dalton Trans.*, 2010, **39**, 2697–2700.
- 13 R. Jothibas, H. V. Huynh and L. L. Koh, *J. Organomet. Chem.*, 2008, **693**, 374–380.
- 14 S. Gaillard, A. M. Z. Slawin, A. T. Bonura, E. D. Stevens and S. P. Nolan, *Organometallics*, 2009, **29**, 394–402.
- 15 M. C. Jahnke, T. Pape and F. E. Hahn, *Z. Anorg. Allg. Chem.*, 2010, **636**, 2309–2314.
- 16 M. Pažický, A. Loos, M. J. Ferreira, D. Serra, N. Vinokurov, F. Rominger, C. Jäkel, A. S. K. Hashmi and M. Limbach, *Organometallics*, 2010, **29**, 4448–4458.
- 17 C. Hirtenlehner, C. Krims, J. Hölbling, M. List, M. Zabel, M. Fleck, R. J. Berger, W. Schoefberger and U. Monkowius, *Dalton Trans.*, 2011, **40**, 9899–9910.
- 18 S. Gaillard, X. Bantreil, A. M. Slawin and S. P. Nolan, *Dalton Trans.*, 2009, 6967–6971.
- 19 M. Kriechbaum, D. Otte, M. List and U. Monkowius, *Dalton Trans.*, 2014, **43**, 8781–8791.
- 20 A. Collado, J. Bohnenberger, M. J. Oliva-Madrid, P. Nun, D. B. Cordes, A. M. Slawin and S. P. Nolan, *Eur. J. Inorg. Chem.*, 2016, **2016**, 4111–4122.
- 21 J. Gil-Rubio, V. Cámara, D. Bautista and J. Vicente, *Inorg. Chem.*, 2013, **52**, 4071–4083.
- 22 W. Liu, K. Bensdorf, M. Proetto, A. Hagenbach, U. Abram and R. Gust, *J. Med. Chem.*, 2012, **55**, 3713–3724.
- 23 H. Sivaram, J. Tan and H. V. Huynh, *Organometallics*, 2012, **31**, 5875–5883.
- 24 C. Topf, C. Hirtenlehner, M. Zabel, M. List, M. Fleck and U. Monkowius, *Organometallics*, 2011, **30**, 2755–2764.
- 25 M. Muuronen, J. E. Perea-Buceta, M. Nieger, M. Patzschke and J. Helaja, *Organometallics*, 2012, **31**, 4320–4330.
- 26 J. P. Reeds, A. C. Whitwood, M. P. Healy and I. J. Fairlamb, *Organometallics*, 2013, **32**, 3108–3120.
- 27 C. Topf, C. Hirtenlehner, M. Fleck, M. List and U. Monkowius, *Z. Anorg. Allg. Chem.*, 2011, **637**, 2129–2134.
- 28 C. Hemmert, R. Poteau, M. Laurent and H. Gornitzka, *J. Organomet. Chem.*, 2013, **745**, 242–250.
- 29 F. dit Dominique, H. Gornitzka, A. Sournia-Saquet and C. Hemmert, *Dalton Trans.*, 2009, 340–352.
- 30 M. Baron, C. Tubaro, M. Basato, A. A. Isse, A. Gennaro, L. Cavallo, C. Graiff, A. Dolmella, L. Falivene and L. Caporaso, *Chem. – Eur. J.*, 2016, **22**, 10211–10224.
- 31 C. Tubaro, M. Baron, M. Costante, M. Basato, A. Biffis, A. Gennaro, A. A. Isse, C. Graiff and G. Accorsi, *Dalton Trans.*, 2013, **42**, 10952–10963.
- 32 Z. Lu, S. A. Cramer and D. M. Jenkins, *Chem. Sci.*, 2012, **3**, 3081–3087.
- 33 G. Marangoni, B. Pitteri, V. Bertolasi, G. Gilli and V. Ferretti, *J. Chem. Soc., Dalton Trans.*, 1986, 1941–1944.
- 34 V. Duckworth and N. Stephenson, *Inorg. Chem.*, 1969, **8**, 1661–1664.
- 35 H. V. Huynh, S. Guo and W. Wu, *Organometallics*, 2013, **32**, 4591–4600.
- 36 G. Nardin, L. Randaccio, G. Annibale, G. Natile and B. Pitteri, *J. Chem. Soc., Dalton Trans.*, 1980, 220–223.
- 37 L. S. Hollis and S. J. Lippard, *J. Am. Chem. Soc.*, 1983, **105**, 4293–4299.
- 38 M. P. Suh, I. S. Kim, B. Y. Shim, D. Hong and T.-S. Yoon, *Inorg. Chem.*, 1996, **35**, 3595–3598.
- 39 S. Alvarez, *Dalton Trans.*, 2013, **42**, 8617–8636.
- 40 R. Elder and J. Watkins, *Inorg. Chem.*, 1986, **25**, 223–226.
- 41 H. Isci and W. R. Mason, *Inorg. Chem.*, 1983, **22**, 2266–2272.
- 42 S. Ramalingam and S. Soundararajan, *J. Inorg. Nucl. Chem.*, 1967, **29**, 1763–1768.
- 43 W. J. Geary, *Coord. Chem. Rev.*, 1971, **7**, 81–122.
- 44 C. B. Aakeröy, T. A. Evans, K. R. Seddon and I. Pálinkó, *New J. Chem.*, 1999, **23**, 145–152.
- 45 B. Jacques, D. Hueber, S. Hameury, P. Braunstein, P. Pale, A. I. Blanc and P. de Frémont, *Organometallics*, 2014, **33**, 2326–2335.
- 46 J. L. Hickey, PhD thesis, The University of Western Australia, 2008.
- 47 M. Baron, C. Tubaro, M. Basato, A. Biffis and C. Graiff, *J. Organomet. Chem.*, 2012, **714**, 41–46.
- 48 J. L. Wong and J. H. Keck Jr., *J. Org. Chem.*, 1974, **39**, 2398–2403.



- 49 Y. Takeuchi, H. J. Yeh, K. L. Kirk and L. A. Cohen, *J. Org. Chem.*, 1978, **43**, 3565–3570.
- 50 C. Hardacre, J. D. Holbrey and S. J. McMath, *Chem. Commun.*, 2001, 367–368.
- 51 M. V. Baker, B. W. Skelton, A. H. White and C. C. Williams, *Organometallics*, 2002, **21**, 2674–2678.
- 52 M. V. Baker, M. J. Bosnich, D. H. Brown, L. T. Byrne, V. J. Hesler, B. W. Skelton, A. H. White and C. C. Williams, *J. Org. Chem.*, 2004, **69**, 7640–7652.
- 53 M. V. Baker, D. H. Brown, C. H. Heath, B. W. Skelton, A. H. White and C. C. Williams, *J. Org. Chem.*, 2008, **73**, 9340–9352.
- 54 M. Baron, C. Tubaro, A. Biffis, M. Basato, C. Graiff, A. Poater, L. Cavallo, N. Armaroli and G. Accorsi, *Inorg. Chem.*, 2012, **51**, 1778–1784.
- 55 Y. Unger, A. Zeller, M. A. Taige and T. Strassner, *Dalton Trans.*, 2009, 4786–4794.
- 56 O. Sanchez, S. González, M. Fernández, A. R. Higuera-Padilla, Y. Leon, D. Coll, A. Vidal, P. Taylor, I. Urdanibia and M. C. Goite, *Inorg. Chim. Acta*, 2015, **437**, 143–151.
- 57 T. Pape and F. E. Hahn, *Dalton Trans.*, 2013, **42**, 7330–7337.
- 58 G. M. Sheldrick, *Acta Crystallogr., Sect. C: Struct. Chem.*, 2015, **71**, 3–8.

